International Journal for Parasitology: Drugs and Drug Resistance 6 (2016) 154–164

Contents lists available at ScienceDirect

International Journal for Parasitology: Drugs and Drug Resistance

journal homepage: www.elsevier.com/locate/ijppaw

Interactions between 4-aminoquinoline and heme: Promising mechanism against *Trypanosoma cruzi*

Guilherme Curty Lechuga [a], Júlio Cesar Borges [b, c], Claudia Magalhães Calvet [d], Humberto Pinheiro de Araújo [e], Aline Araujo Zuma [f], Samara Braga do Nascimento [a], Maria Cristina Machado Motta [f], Alice Maria Rolim Bernardino [c], Mirian Claudia de Souza Pereira [d, *, 1], Saulo Cabral Bourguignon [a, **, 1]

[a] *Laboratório de Interação celular e molecular, Departamento de Biologia Celular e Molecular, Universidade Federal Fluminense, Rua Outeiro São João Batista, 24020-141, Niterói, Rio de Janeiro, Brazil*
[b] *Departamento de Química Orgânica, Universidade Federal Fluminense, Rua Outeiro São João Batista, 24020-141, Niterói, Rio de Janeiro, Brazil*
[c] *Instituto Federal de Educação, Ciência e Tecnologia do Rio de Janeiro, Campus Nilópolis, 26530-060, RJ, Brazil*
[d] *Laboratório de Ultraestrutura Celular, Instituto Oswaldo Cruz, Fundação Oswaldo Cruz, Avenida Brasil 4365, 21040-360, Rio de Janeiro, RJ, Brazil*
[e] *Departamento de Imunologia, Instituto Nacional de Controle de Qualidade em Saúde, Fundação Oswaldo Cruz, Avenida Brasil 4365, 21040-360, Rio de Janeiro, RJ, Brazil*
[f] *Laboratório de Ultraestrutura Celular Hertha Meyer, Instituto de Biofísica Carlos Chagas Filho, Universidade Federal do Rio de Janeiro, Avenida Carlos Chagas Filho, 373-bloco G. Cidade Universitária, Ilha do Fundão, Rio de Janeiro, RJ, Brazil*

ARTICLE INFO

Article history:
Received 2 December 2015
Received in revised form
25 June 2016
Accepted 12 July 2016
Available online 14 July 2016

Keywords:
Quinoline
Heme
Trypanosoma cruzi
Chemotherapy
Chagas disease

ABSTRACT

Chagas disease is a neglected tropical disease caused by the flagellated protozoan *Trypanosoma cruzi*. The current drugs used to treat this disease have limited efficacy and produce severe side effects. Quinolines, nitrogen heterocycle compounds that form complexes with heme, have a broad spectrum of anti-protozoal activity and are a promising class of new compounds for Chagas disease chemotherapy. In this study, we evaluated the activity of a series of 4-arylaminoquinoline-3-carbonitrile derivatives against all forms of *Trypanosoma cruzi in vitro*. Compound 1**g** showed promising activity against epimastigote forms when combined with hemin (IC50<1 μM), with better performance than benznidazole, the reference drug. This compound also inhibited the viability of trypomastigotes and intracellular amastigotes. The potency of 1**g** in combination with heme was enhanced against epimastigotes and trypomastigotes, suggesting a similar mechanism of action that occurs in *Plasmodium* spp. The addition of hemin to the culture medium increased trypanocidal activity of analog 1**g** without changing the cytotoxicity of the host cell, reaching an IC50 of 11.7 μM for trypomastigotes. The mechanism of action was demonstrated by the interaction of compound **1g** with hemin in solution and prevention of heme peroxidation. Compound 1**g** and heme treatment induced alterations of the mitochondrion-kinetoplast complex in epimastigotes and trypomastigotes and also, accumulation of electron-dense deposits in amastigotes as visualized by transmission electron microscopy. The trypanocidal activity of 4-aminoquinolines and the elucidation of the mechanism involving interaction with heme is a neglected field of research, given the parasite's lack of heme biosynthetic pathway and the importance of this cofactor for parasite survival and growth. The results of this study can improve and guide rational drug development and combination treatment strategies.

1. Introduction

Neglected diseases caused by protozoan parasites affect social and productive life of millions of people worldwide (Conteh et al., 2010), causing a substantial economic burden. Chagas disease, a neglected tropical disease caused by the flagellated protozoan

* Corresponding author.
** Corresponding author.
E-mail addresses: mirian@ioc.fiocruz.br (M.C.S. Pereira), saulocb@globo.com (S.C. Bourguignon).
[1] These authors contributed equally to this work.

http://dx.doi.org/10.1016/j.ijpddr.2016.07.001

Trypanosoma cruzi, is an example of a devastating illness that affects approximately 6–7 million people in Latin America (WHO, 2015). *T. cruzi* is naturally transmitted in rural endemic areas by triatomines, but the current scenario shows the spread of Chagas disease to non-endemic countries due to blood transfusion and organ transplantation from infected immigrants (Coura and Vinas, 2010). Thus, the disease is emerging as a global public health problem with an eminent economic impact (Vannucchi et al., 2014). This silent disease is divided into two clinical phases: an acute phase, characterized by parasitemia and nonspecific symptoms, and chronic phase, which can be asymptomatic or may lead to cardiac, neurological and digestive disorders (Rassi and Marin-Neto, 2010). The currently available drugs, nifurtimox and benznidazole (Bz), have limitation in the acute phase due to parasite natural resistance, cause severe side effects and present no efficacy in chronic phase of Chagas disease (Coura and Castro, 2002; Meeks et al., 2015).

The therapeutic failure of promising drugs that were in advanced clinical trials (Molina et al., 2014) makes the search for new effective compounds, targets and lead optimization essential for effective therapy of Chagas disease. A rational strategy for drug development is to seek metabolic targets critical for parasite survival or molecules that have already shown a wide spectrum of antiprotozoal activity.

Quinoline derivatives are well-known for their important anti-*Plasmodium* activity, and therefore, represent a class of drugs for malaria treatment (Foley and Tilley, 1998). However, these substances have many other pharmacological activities against *Leishmania* spp. (Nakayama et al., 2007; Tiuman et al., 2011), trypanosomes (Kinnamon et al., 1996; Muscia et al., 2011), bacteria (Eswaran et al., 2010) and tumors (Ganguly et al., 2011). The mechanism of action of quinoline drugs in *Plasmodium* spp. is based on the formation of quinoline-heme complexes that are responsible for inhibiting heme crystalization into hemozoin, leading to high levels of free heme and inducing pro-oxidant effects that culminate in parasite death (Foley and Tilley, 1998). Heme is a fundamental molecule for biological processes functioning as a cofactor for proteins involved in the transport and storage of oxygen, electron transport in mitochondria (complexes II-IV), drug and steroid metabolism (cytochromes), signal transduction and regulation of antioxidant enzymes (Tripodi et al., 2011). However, *T. cruzi* lacks the heme biosynthetic pathway and needs to import this molecule from both vertebrate and invertebrate hosts. After heme uptake, it is distributed to subcellular compartments (Cupello et al., 2011) and although this delivery process is not well understood, it seems that heme-proteins, such as cytochromes, participate in essential metabolic pathways in the parasite (Choi et al., 2013). Thus, the formation of heme-quinolines may be a promising strategy for interfering with the heme metabolism in *T. cruzi*.

The present paper demonstrates the activity of 4-aminoquinoline derivatives against *T. cruzi* and shows that combination treatment with hemin produces a synergic effect enhancing trypanocidal activity. These results emphasize the potential use of quinolines as promising candidates for lead compounds against *T. cruzi*.

2. Material and methods

2.1. Chemistry

Preparation of the 4-arylaminoquinoline-3-carbonitrile derivatives: 1.0 mmol of 4-chloroquinolines (2) and 1.5 mmol of corresponding aniline were stirred in 6.0 mL of diethyleneglycol at 120 °C for 1 h. Finally, the mixture was placed in a beaker of ice and water. The crystals formed were filtered and recrystalized in ethanol (Borges et al., 2014; Leal et al., 2008). Subsequently, all compounds formed (**1a**–**1g**) were identified by ^{1}H NMR, ^{13}C NMR and FT-IR spectroscopies (Supplementary Material).

2.2. Cell culture and cytotoxicity assays

Heart muscle cells were enzymatically isolated from mice embryo myocardia, as described previously (Meirelles et al., 1986). Cardiomyocytes (CM) were cultivated in Dulbecco's modified Eagle medium (DMEM), supplemented with 2.5 mM $CaCl_2$, 2% chick embryo extract, 7% fetal bovine serum (FBS), 1 mM L-glutamine and antibiotics. The cells were maintained at 37 °C in a 5% CO_2 atmosphere and the culture medium was changed every 2 days. Vero cells (ATCC® CCL-81™) were cultivated in RPMI 1640 medium supplemented with 10% of FBS and maintained at 37 °C in a 5% CO_2 atmosphere. All procedures involving animals were approved by the Committee of Ethics for the Use of Animals from FIOCRUZ (CEUA LW-37/13).

Vero cells and cardiomyocytes were used to analyze the cytotoxic effects of the quinoline derivatives (**1a**–**1g**), according to the modified procedures described previously (de Menezes et al., 2015). Briefly, Vero cells and CM were seeded at 1.5×10^4 and 7×10^4 cells per well in 96-well microplates, respectively. After 24 h of culture, cells were treated with compound concentrations ranging from 100 to 3.7 μM for 72 h at 37 °C in a 5% CO_2 atmosphere. Cell viability was analyzed by adding 50μL/well of resazurin solution (0.005%) followed by incubation for 4 h at 37 °C, as a metabolic indicator. Fluorescence intensity was measured at 530 nm and 600 nm using SpectraMax M2 microplate reader (Molecular Devices, Sunnyvale, CA). The compound inhibitory concentration that reduces 50% of cell viability (CC50) was determined by fitting the dose-response curve compared to untreated control.

2.3. Parasites

T. cruzi Y epimastigote forms were cultivated at 28 °C in BHI broth medium supplemented with folic acid, hemin (150 μM), and 10% FBS. All experimental assays were performed with parasites in log phase of growth (Carneiro et al., 2012). Bloodstream trypomastigotes of Y strain were isolated from *Swiss Webster* mice infected with *T. cruzi* at the peak of parasitaemia (Meirelles et al., 1984). Culture-derived trypomastigotes (Y strain) were isolated from the supernatant of *T. cruzi*-infected Vero cultures at 4 days post-infection (dpi).

2.4. Antiparasitic activity

To analyze the effect of quinolines (**1a**–**1g**), *T. cruzi* Y epimastigote forms (5×10^5 parasites/mL) were treated with different compound concentrations (50, 25 and 12.5 μM) in supplemented BHI medium for 72 h. The compounds were stored at a maximum 10 mM stock solution in dimethyl sulfoxide (DMSO) and the final solvent concentration never exceeded the non-toxic concentration (1%). The interference of heme on the parasite proliferation was determined by treating the parasites for 72 h with different concentration (50, 12.5 and 6.25 μM). Prior to compound treatment, the epimastigotes were washed twice in PBS and then incubated with the selected effective compounds in BHI medium with or without heme (hemin 30 μM). The effect of treatment in epimastigote growth was determined by counting the total parasites/mL in a Neubauer chamber and the IC50 (concentration that inhibits 50% of parasite growth) was calculated using probits. Morphology and motility were used as parameters for viability. As control, the growth curve was performed in BHI medium containing 1% DMSO.

Culture-derived trypomastigotes (2×10^6 parasites/100 μl) of Y

strain were incubated for 24 h at 37 °C with 30 μM of quinoline derivatives (1**a**-1**g**) and Bz. The synergic effect of quinolines and heme was evaluated by adding 30 μM of hemin in RPMI 1640 medium. Additionally, the IC50 (compound concentration that reduces 50% of parasite viability) was calculated by treating trypomastigotes with the selected quinoline and Bz (100–1.2 μM) for 24 h. The efficacy of combined substances (quinolines and hemin) was evaluated by adding resazurin solution (0.005%) as described above. Fluorescence intensity was measured at 530 nm and 600 nm with SpectraMax M2 microplate reader (Molecular Devices, Sunnyvale, CA). Parasite counting was also performed but no difference in IC50 values was observed (data not included). Percentage of cell death was calculated using the correspondent control (untreated or hemin treated trypomastigotes).

Primary cultures of cardiomyocytes were used for screening the activity of quinolines on intracellular amastigotes. Cardiomyocytes, a target cell of *T. cruzi* infection, were seeded (1.2×10^5 cells/well) in 24-well culture plates containing 13 mm^2 glass coverslips and, after 24 h of culture, the cells were infected with bloodstream trypomastigotes (Y strain) at a ratio of 10:1 parasites-host cell. After 24 h of interaction, free trypomastigotes were removed by washing with Ringer's solution (154 mM NaCl, 56 mM KCl, 17 mM Na_2HPO_4, pH 7.0) and then, cells were incubated for 72 h with 10 μM of Bz and compounds (1**a**–1**g**). Bz and the most potent quinoline were selected and tested at different concentrations (30, 15 and 7.5 μM) in combination with hemin (30 μM). After washing, the samples were fixed in Bouin's solution followed by staining with Giemsa. Counts were performed in order to obtain the endocytic index (EI) and IC50. Thus, the percentage of infected cells and the total number of intracellular parasites were determined by random quantification of at least 200 cells from each replicate. EI was calculated by the percentage of infected cell multiplied by the average number of intracellular parasites per infected host cell. Three different assays were performed in duplicate.

2.5. Propidium iodide exclusion assay

Flow cytometry analysis was used to examine the effect of compound 1**g** and its combined treatment with hemin on the parasite viability. *T. cruzi* epimastigotes of the Y strain were incubated for 96 h with 50 μM of the effective compound in BHI medium with or without 30 μM of heme. The viability of parasites was analyzed using propidium iodide dye, as previously described (Carneiro et al., 2012).

2.6. Ultrastructural analysis

The effect of combined treatment against *T. cruzi* (Y strain) was evaluated by transmission electron microscopy (TEM). Trypomastigotes (2×10^7) were incubated for 24 h with 10 μM of compound 1**g** (IC50) combined with 30 μM of hemin in RPMI medium. Epimastigotes (10^6 parasites/mL) were treated for 72 h with 5 μM of the compound 1**g** (IC75) in BHI medium supplemented with hemin (30 μM). After incubation, parasites were washed three times with PBS and fixed for 1 h at 4 °C with 2.5% glutaraldehyde (GA) in 0.1 M sodium cacodylate buffer, pH 7.2, followed by post-fixation for 1 h at 4 °C with 1% OsO_4.

Additionally, uninfected and *T. cruzi*-infected cardiomyocyte cultures were treated for 72 h with hemin (30 μM) or the IC50 and IC75 concentration of compound 1**g** in combination with hemin (30 μM). Subsequently, the cultures were fixed with 2.5% GA and post-fixed in the presence of 0.8% potassium ferrocyanide to enhance membrane contrast, as described above. Both samples, parasites and cardiomyocyte cultures, were dehydrated in serial graded acetone batches impregnated and embedded in Epon 812. Ultrathin sections were stained with 5% uranyl acetate and 2% lead citrate and subsequently examined in a JEOL transmission electron microscope (JEM1011).

2.7. Quinoline inhibition of heme peroxidation

The assays were preformed following procedures previously described (Sonnet and Mullie, 2011). Briefly, a total of 20 μl of daily prepared hemin stock solution (300 μM in 0.1 M NaOH) was added to 180 μl of BSA (1 mg/ml) in 0.2 M sodium acetate (pH = 5.2) or 20 mM phosphate buffer (pH = 7.4) in 96-well plate. To analyze the effect on heme peroxidation, different concentrations of compound 1**g** (100, 50 and 25 μM) were added to this solution and the reaction of hemin peroxidation was initiated by adding 20 μl of H_2O_2 (200 μM). After 1 h of incubation, the absorbance of Soret band (405 nm) was measured with a microplate reader (TP reader). The solvent of the compound (DMSO 1%) was used as control. For negative controls, H_2O was added instead of H_2O_2. Results were expressed as percentage of non-degraded hemin in solution.

2.8. Hemin binding assay

Hemin stock solution was freshly prepared at 10 mM in 0.1 M NaOH and stored at 4 °C (protected from light). Hemin was diluted at 10 μM of final concentration in 20 mM phosphate buffer (pH 7.4). Subsequently, different concentrations of compound 1**g** (25, 10 and 5 μM) were added to the solution. UV/Vis absorption spectra of hemin was measured with the SpectraMax M2 spectrophotometer (Molecular Devices, Sunnyvale, CA), at 25 °C using a quartz cuvette. The measurements were performed in the range of 300–700 nm with 5 nm of increment. DMSO (0.25%) the solvent of compounds was used as control.

2.9. Statistical analysis

Mann-Whitney test, one and two-way ANOVA (Bonferroni post test) on Graphpad Prism 5.0 and the Student *t*-test were used for statistical analysis. Value of $p \leq 0.05$ was considered statistically significant. The data were expressed as mean ± standard deviation.

3. Results

A series of seven 4-arylaminoquinoline-3-carbonitrile derivatives **(1a–g)** were prepared through the reaction of 4-chloroquinolines-3-carbonitriles with anilines using diethylene glycol as a solvent. The chlorine atom in the position 4 can be easily replaced by nucleophiles, such as anilines in a nucleophilic aromatic substitution (Leal et al., 2008). As shown in Fig. 1, the 4-chloroquinolines were quickly prepared from 4-oxo-1,4-dihydroquinolines-3-carbonitriles using a methodology described by Gould-Jacobs and co-workers (Borges et al., 2014).

The synthetic compounds were first screened against epimastigote forms of *T. cruzi* in order to evaluate their antiparasitic activity. Substances were synthesized preserving the quinolinic structure of the drug amodiaquine. Several substituent groups were added to the phenylamino ring such as halogens and methoxy, which differentially affected the parasites. Although all analogs showed activity against epimastigotes with IC50s ranging from 0.9 to 40 μM (Table 1), only compound 1**g** was more effective than benznidazole (Bz), the reference drug, for which the IC50 was 5.6 μM. Furthermore, compound 1**g** achieved the greatest selectivity index (SI) among all quinolines tested (Table 1). Additionally, the screening of quinoline compounds (10 μM) against intracellular amastigotes also revealed a better activity of compound 1**g**, achieving 64% inhibition of amastigote growth (Table 1).

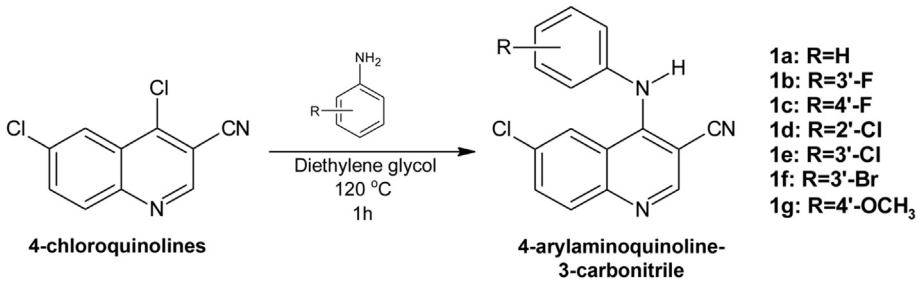

Fig. 1. General scheme of quinolines (1**a**–1**g**) synthesis. Products were identified by ^{1}H NMR, ^{13}C NMR, FT-IR spectroscopies.

Table 1
In vitro cytotoxicity and anti-proliferative effect of quinoline derivatives against epimastigotes and amastigotes.

Compounds	CC50[a]	CC50[b]	IC50[c]	SI[d]	% inhibition[e]
Bz	>100	>100	5.6 ± 0.05	>17.85	99.8 ± 0.4
1a	>100	>100	17.6 ± 6.1	>5.68	45.5 ± 9
1b	69 ± 22	67 ± 11.6	16.6 ± 0.2	4	53.2 ± 10
1c	>100	>100	8.8 ± 1.3	>11.36	52.5 ± 6
1d	64 ± 12.5	47.7 ± 13	40 ± 13.7	1.19	57.6 ± 8
1e	89 ± 18	65.2 ± 18.5	15.4 ± 0.7	4.2	55.4 ± 7
1f	71 ± 26	>100	21.2 ± 14.2	>4.7	60.4 ± 9
1g	>100	>100	0.9 ± 1.2	>111.1	64.5 ± 2

CC_{50} (Cytotoxicity concentration that kills 50% of the host cells) of Vero cells[a] and cardiomyocytes[b] calculated using dose response curve. Results of mean and standard deviation of the assays in triplicates. Control corresponds of 100% of living cells without the compounds.
[c]IC_{50} (Concentration that inhibits the growth of 50% of *T. cruzi* Y epimastigote forms within 72 h) calculated using Probit. The drug activity was performed in the presence of 150 μM of heme.
[d]SI (Selective index = CC50 (Cardiomyocytes)/IC50).
[e]Percentage of amastigote growth inhibition after 72 h of treatment with 10 μM of compounds. Results represent the mean and standard deviation of three assays in duplicates.

Based on the quinoline mechanism of action on *Plasmodium* spp., one open question was whether heme plays an important role in the activity of these compounds on *T. cruzi*. Therefore, analyses were undertaken of the direct effect of quinoline derivatives on the parasites in the presence or absence of heme. For tests with epimastigotes and trypomastigotes, hemin was added at the concentration of 30 μM in BHI and RPMI 1640 medium, respectively. The screening of quinolines activity (30 μM) against trypomastigotes, assessed by using resazurin viability assay, revealed that compound activity was significantly increased in combination with 30 μM of hemin, including Bz (Fig. 2). No difference in trypomastigote death was found in control groups. Although a small increase of about 1.3 and 1.6 fold has been observed in the activity of Bz and quinoline 1**a**, respectively (Fig. 2), addition of hemin did not improve Bz activity (Table 2). The combined treatment with quinolines (1**b**–1**g**) deeply increased the death of trypomastigote forms, raising the activity from 9 to 41-fold (Fig. 2).

Compound 1**g** was selected for further analysis because it had greater action against proliferative forms. Our findings demonstrated a potentialized effect of compound 1**g** associated with heme. The removal of hemin reduced the activity of the compound 1**g** leading to an increase of IC50 value in epimastigotes (IC50 = 19.5 μM) (Table 2). Trypomastigotes were also more sensitive to the combined treatment (IC50 = 11.7 μM). These data showed that heme promoted a ~21-fold and ~8-fold enhancement of compound activity in epimastigotes and trypomastigotes, respectively, when compared to treated parasites without hemin (Table 2). Enhancement of Bz activity was not noticed in the presence of hemin for all development stages (Table 2).

Since epimastigotes are one of the proliferative stages of *T. cruzi*, we were interested in determining whether the reduction in the number of epimastigotes after treatment with compound 1**g** was due to growth inhibition or cell death. A dose response growth curve of epimastigotes cultivated in the presence of 1**g** or its combination with heme (hemin 30 μM) was evaluated up to 72 h (Fig. 2). Interestingly, all concentrations of the compounds tested (50, 12.5 and 6.25 μM) seem to inhibit parasite proliferation in the presence of hemin, whereas only the highest concentration of 1**g** (50 μM) was active against the parasites in the absence of heme (Fig. 2A and B), demonstrating that the association with heme amplifies the mechanism of action of this compound. In fact, flow cytometry analysis, using propidium iodide dye, revealed that the combined treatment (heme plus 50 μM of 1**g**) elicited intense cell death (80% by 96 h), which was 4.6-fold higher than without hemin (Fig. 2C).

Compound 1**g** was also selected to proceed combined treatment against intracellular forms. Our results demonstrated that addition of hemin (30 μM) did not potentiate the efficacy of the compound as occurred for epimastigotes and trypomastigotes (Table 2). Concentrations ≥15 μM of the compound 1**g** lead to a reduction of approximately 70% of the endocytic index, independently of heme combination (Fig. 3). The IC50 achieved with compound 1**g** alone (IC50 = 12 μM) was approximately two times higher than the combined treated group (IC50 = 6.3 μM). Although compound 1**g** has demonstrated activity against amastigotes, showing no drastic shift in IC50 in the presence of hemin, it was not as effective as Bz (Table 2). Light microscopy analysis revealed an intense reduction in infection profile after treatment of *T. cruzi*-infected cardiomyocyte cultures with Bz. In contrast, no effect was observed after treatment with compound 1**g** (7.5 μM) alone while combined treatment reduced the number of intracellular parasites (Fig. 3).

The remarkable change in the activity profile of the compound 1**g** in the presence of heme led to questions about the molecular interactions between these two substances. Then, the ability of the compound 1**g** to inhibit the hemin peroxidation was evaluated using a spectrophotometric method (Sonnet and Mullie, 2011). Hydrogen peroxide (H_2O_2) breaks heme and reduces the Soret band, which is a characteristic of substances that have heme and, therefore, can be quantified by spectrophotometry. One striking feature was the prevention of heme peroxidation in the presence of compound 1**g** in acid and neutral pH (Fig. 4). Compound concentrations ≥50 μM were capable of protecting the heme from the H_2O_2 effect in both acetate and phosphate buffers. In acid pH (pH 5.2), the addition of 1**g** enhanced the protective effect of heme peroxidation in all concentrations analyzed (Fig. 4), resulting in a maximal protection of 91.8% at 100 μM as compared to control. The same concentration at neutral pH also inhibited H_2O_2 effect, showing 68% of unchanged hemin (Fig. 4).

UV/Vis absorption spectroscopy was used to evaluate the interactions between compound 1**g** and hemin in solution. To mimic

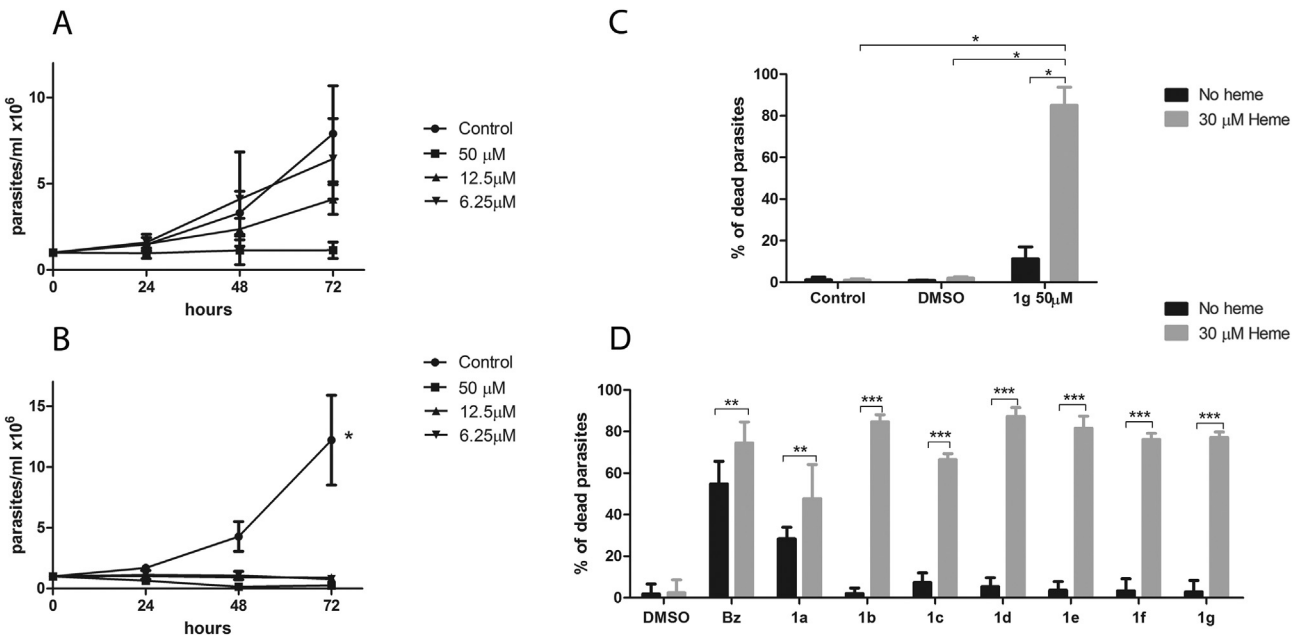

Fig. 2. Effect of quinoline derivatives against *T. cruzi*. Growth curve of *T. cruzi* epimastigotes treated with different concentrations of 1**g** in medium without hemin supplementation (A) or supplemented with 30 μM of hemin (B). Propidium iodide staining of epimastigotes treated for 96 h with 50 μM of 1**g** in medium supplemented or not with 30 μM of hemin (C). The activity of the compound 1**g** was clearly raised in the presence of hemin, which increased parasite death rates. Viability of trypomastigote forms was demonstrated by resazurin assay after 24 h of treatment with 30 μM of quinolines (1**a**–1**g**) and Bz combined or not with 30 μM of hemin. Note that combined treatment (quinolines + hemin) increased the activity of all compounds against trypomastigotes but the quinoline series (1**b**–1**g**) were mostly improved compared to compound 1**a** and Bz (D). Results represent the mean and standard deviation of three independent experiments in duplicate. Difference between groups was analyzed with two-way ANOVA, Bonferroni post test. *Statistically significant $p \leq 0.05$, **Statistically significant $p \leq 0.01$ and ***Statistically significant $p \leq 0.001$.

Table 2
IC50 of Bz and 1g on epimastigotes (Epi), trypomastigotes (Tryp) amastigotes (Ama), Vero cells and Cardiomyocytes (Vero/CM) incubated in medium with and without hemin. Results represent the mean and standard deviation of at least three experiments in duplicate.

Medium	1g				Bz			
	Epi[a]	Tryp[b]	Ama[c]	Vero/CM[d]	Epi[a]	Tryp[b]	Ama[c]	Vero/CM[d]
Without heme	19.5 ± 2.5	>100	12.2 ± 2.6	>100	2.9 ± 0.6	13 ± 5.7	3.25 ± 0.3	>100
With heme*	<1**	11.7 ± 4**	6.3 ± 2.5**	>100	9.5 ± 5.2**	12 ± 6.5	2.5 ± 1.4	>100

*30 μM of heme diluted in BHI, RPMI and DMEM medium.
**Statistically significant $p < 0.05$ using one-way ANOVA.
[a] IC_{50} (Concentration that inhibits the growth of 50% of *T. cruzi* Y epimastigote forms within 72 h). Viability was measure counting motile parasites in Neubauer chamber.
[b] IC_{50} (Concentration that kills 50% of *T. cruzi* Y trypomastigotes within 24 h). Viability was measure using resazurin.
[c] IC_{50} (Concentration that inhibits 50% of *T. cruzi* Y amastigotes after 72 h of treatment). Measured by counting the number of parasites stained with GIEMSA.
[d] CC_{50} (Concentration that inhibits 50% of host cell growth after 72 h of treatment). Viability was measure using resazurin.

cellular environment in cultured medium a neutral pH (7.4) was chosen. In phosphate buffer a broad Soret band with a peak around 385 nm was observed. The addition of 1**g** produced spectral alterations like shift and decrease of the Soret band (Fig. 4), demonstrating a complex formation between heme and 1**g**.

The effect of the combined substances on *T. cruzi* was also evaluated by transmission electron microscopy (TEM). The ultrastructural analysis of untreated epimastigotes demonstrated their characteristic elongated spindle-shaped with cytoplasmic components such as mitochondria, bar-shaped kinetoplast localized anterior to the nucleus, reservosomes and flagellar pocket with emerging flagellum (Fig. 5A). Longitudinal ultrathin-section of trypomastigotes showed the slender shape of the parasite with elongated nucleus, disk-shape kinetoplast visualized posterior to the nucleus, mitochondria and also subpellicular microtubules (Fig. 5B). Treatment of both epimastigotes and trypomastigotes with compound 1**g** combined with 30 μM of hemin revealed changes in the cytoplasmic compartments. An intense kinetoplast swelling with alteration in the distribution and compaction of the kDNA, mitochondrial swelling with disruption of the cristae, and cytoplasmic vacuolization (Fig. 5C–F) were observed in treated parasites, as well as basal body duplication (Fig. 5C) in the non proliferative form of *T. cruzi*. The effect of combined treatment was also evaluated against intracellular amastigotes by TEM. Hemin (30 μM) treatment did not induce ultrastructural changes neither in intracellular forms (Fig. 6B) nor in cardiomyocytes (data not shown). Intracellular forms showed rounded morphology with preserved mitochondria, bar-shaped kinetoplast anterior (amastigotes) or aside (intermediate form) the nucleus as observed in untreated *T. cruzi*-infected cultures (Fig. 6A). Combined treatment (IC50 of compound 1**g** and 30 μM hemin) of infected cultures revealed the presence of few electron-dense deposit associated with membrane profiles within vesicles. (Fig. 6C). Interestingly, an increase in the number of these electron-dense structures in reservosomes was noticed in the posterior region of the parasite after treatment with 1**g** IC75 and hemin (30 μM) (Fig. 6D–F).

4. Discussion

Trypanosoma cruzi needs to overcome environmental changes in

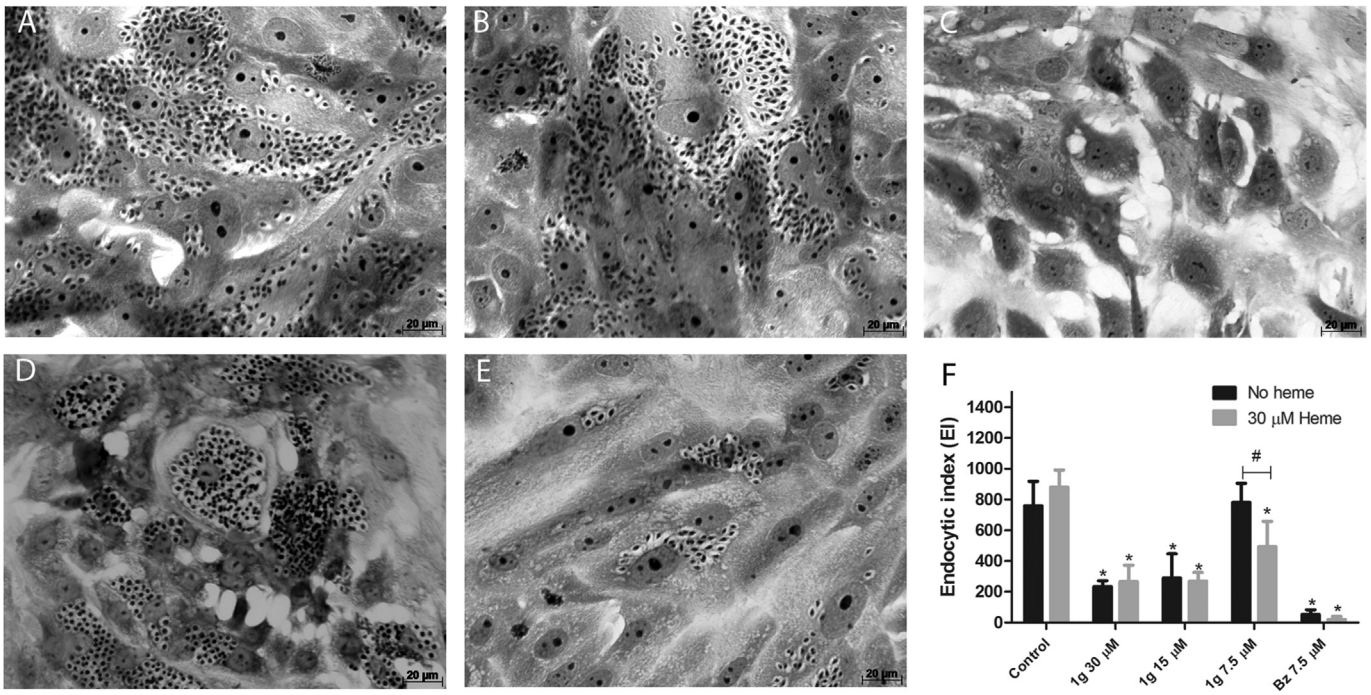

Fig. 3. Light microscopy images of *T. cruzi*-infected cardiomyocytes treated only with quinoline **1g** or combined with hemin. Both negative controls, untreated cardiomyocyte cultures (A) or cultures incubated with 30 μM of hemin (B), showed a high number of intracellular amastigotes after 96 h of infection with *T. cruzi*. (C) Bz treatment (7.5 μM) substantially reduced the *T. cruzi* infection. No change on infection profile was observed in cultures treated with 7.5 μM of compound **1g** (D) while combined treatment with hemin (30 μM) clearly decreased amastigotes nests compared to negative controls and **1g** (7.5 μM) treated cultures (E). (F) The effect of **1g** treatment alone and in combination with hemin (30 μM) on the endocytic index. Although treatment with compound **1g** alone (up to 15 μM) and combined with hemin significantly reduced the endocytic index, the effectiveness was lower than Bz. Note that combined treatment (7.5 μM **1g** and 30 μM hemin) reduced significantly the endocytic ratio when compared to **1g** alone. Data represent mean and standard deviation of experiments in duplicates. *Statistically significant ($p \leq 0.05$), compared to correspondent control using Mann-Whitney test; #Statistically significant ($p \leq 0.05$) using two-way ANOVA. Bars = 20 μm.

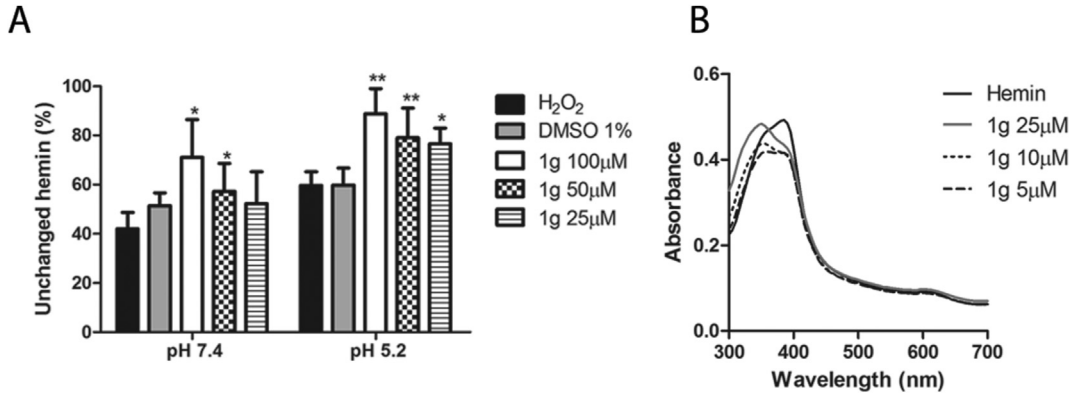

Fig. 4. Peroxidative degradation of hemin. (A) Different concentration of **1g** (100, 50 and 25 μM) inhibit H_2O_2 degradation of hemin at pH 5.2 (acetate buffer) and pH 7.4 (Phosphate buffer). (B) Absorption spectra of hemin in phosphate buffer (pH 7.4) with different concentrations of quinoline **1g** (25, 10 and 5 μM) was recorded over the wavelength range of 300–700 nm, which includes the heme Soret band absorption peak. Interactions in solution with quinoline **1g** and hemin produced a reduction of Soret band. *Statistically significant difference from control at pH 7.4, $p \leq 0.05$; **Statistically significant difference from control at pH 5.2, $p \leq 0.01$.

order to guarantee its development and survival within the insect and mammalian hosts. One striking feature is the rapid adaptation of its metabolism to nutritional changes and aggressive microenvironments (Jimenez, 2014). Heme is a key cofactor in *T. cruzi* metabolism (Lara et al., 2007; Tripodi et al., 2011), but its degradation must be well regulated to prevent damage from uncontrolled oxidative stress (Cupello et al., 2014), resulting in a harmful environment for the parasite. Therefore, the heme metabolism has been highlighted as an important target for drug development.

Quinoline derivatives, which have the property of forming complexes with heme (Egan, 2006; Leed et al., 2002), represent a vast class of antimalarial drugs with a broad spectrum of antiprotozoal activity (Tekwani and Walker, 2006; Upadhayaya et al., 2013). Current evidence strongly supports the use of these drugs in research on Chagas disease, since phenotypic screening of quinoline derivatives has shown a trypanocidal effect and high drug selectivity, supporting their application as lead compounds for drug design against *T. cruzi* (Fonseca-Berzal et al., 2014; Muscia et al., 2011). Our data demonstrate the trypanocidal activity of the quinolines and highlights the potentialized effect of heme combination against *T. cruzi*. The combined treatment improved the **1g** trypanocidal activity by reducing 21, 8 and 2-fold the IC50s in

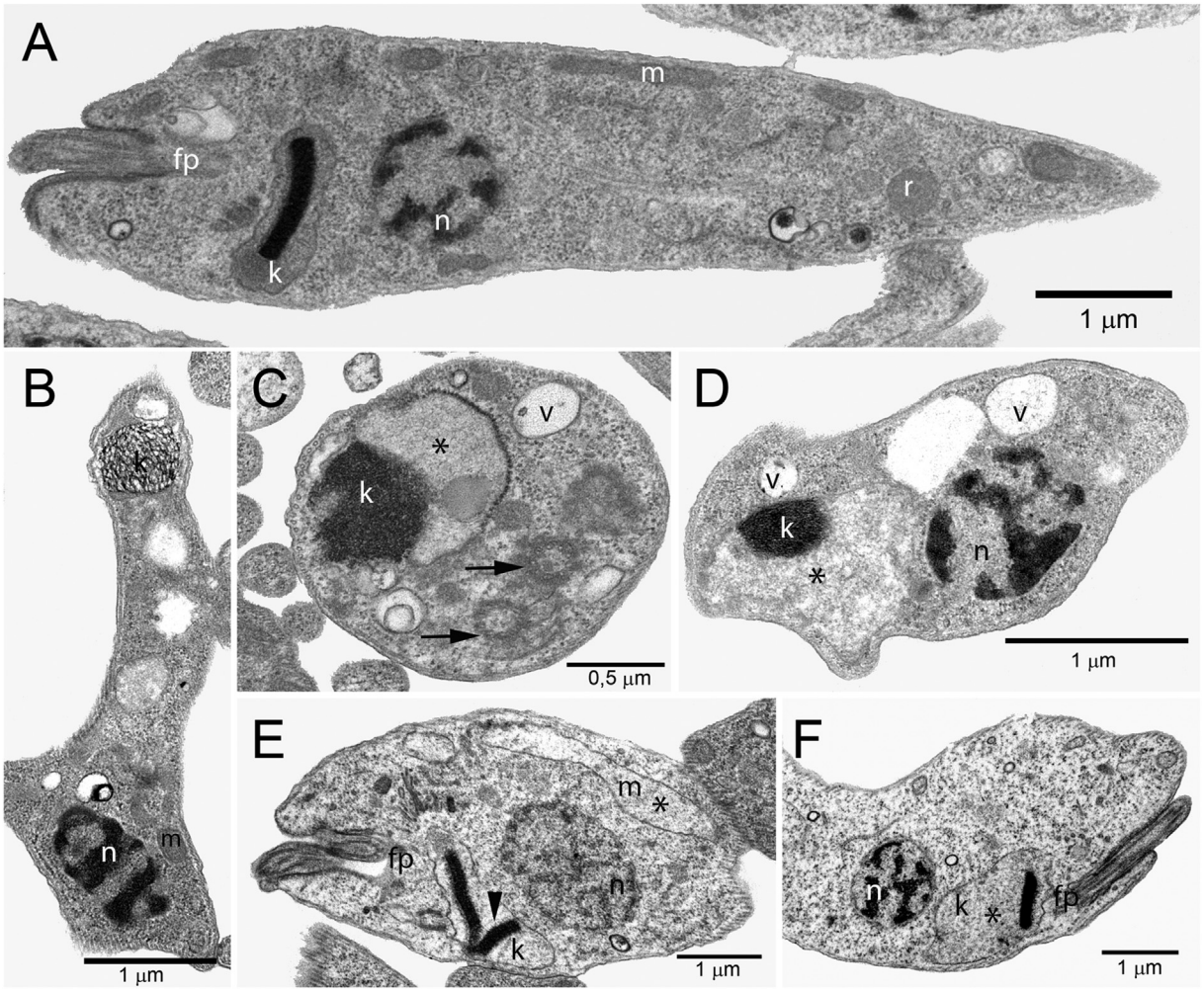

Fig. 5. Transmission electron microscopy of epimastigotes and trypomastigotes treated with quinoline 1**g** combined with heme. (A) Control of epimastigotes cultivated with 30 μM of hemin shows normal morphology of nucleus (n), kinetoplast (k), reservosome (r) and flagellar pocket (fp); (B) Trypomastigotes incubated with 30 μM of heme for 24 h at 37 °C present no alteration on nucleus (n), kinetoplast (k) and mitochondria (m); (C and D) Trypomastigotes treated with compound 1**g** (10 μM) and 30 μM of hemin for 24 h showed an enlargement of the kinetoplast (C; asterisk) with compaction of kDNA (k) and also the presence of vacuoles (v). An unexpected presence of two basal bodies was observed in trypomastigotes, a non-proliferative form of *T. cruzi* (arrows). (E and F) Treatment of epimastigotes for 72 h at 28 °C with 5 μM of compound 1**g** and 30 μM of hemin demonstrated a mitochondrial (m) and kinetoplast (k) swelling (asterisk) and also an atypical distribution of the kDNA network (arrow head). (A,B,D,E and F) Bars = 1 μm; (C) Bars = 0.5 μm.

epimastigote, trypomastigote and amastigote forms of *T. cruzi*, respectively. Molecular changes in quinoline scaffold to improve druglikeness and activity against *T. cruzi* intracellular forms are interesting since quinoline 1**g** fits the criteria for a hit compound against Chagas disease (Don and Ioset, 2014). Furthermore, nanoencapsulation of porphyrins has been considered as a promising strategy to potentialize the antimalarial activity of Zn-protoporphyrin (Alves et al., 2015). Based on the fact that porphyrins cannot easily cross the cell membrane (Krishnamurthy et al., 2007) and intracellular levels of heme are tightly controlled in mammalian cells (Tripodi et al., 2011), drug delivery system may be an important tool to increase permeability of the associated compounds (quinoline and hemin). Further studies will be undertaken to elucidate the fate of heme and its role in the mechanism of action of quinolines in *T. cruzi*. Heme detoxification is essential for *T. cruzi* homeostasis in order to avoid the production of free radicals. *Leishmania* spp., for example, increases the expression of HO-1 to regulate heme participation in superoxide production by impairing $gp91^{phox}$ maturation, a subunit of NADPH oxidase complex, in amastigotes infected macrophages (Pham et al., 2005). Thus, the sequestration of heme, by its association with the quinoline 1**g**, may impair heme degradation and induce oxidative stress, leading to parasite death (Foley and Tilley, 1998).

Ours findings of the inhibition of heme peroxidation and binding assay reinforce the formation of a heme-quinoline complex, which protects heme from H_2O_2 peroxidation. This mechanism is involved in the increasing of oxidative stress by quinoline derivatives, since heme has a catalase-like activity (Loria et al., 1999). Although the formation of the heme-quinoline 1**g** adduct occurs in both alkaline and acid pH, the interaction of the compounds appears to be favored in acidic environments, suggesting that ionization may amplify the interaction between these substances in acid intracellular compartments. Our data correlates with previous study that showed the protective effect of ICL670, an iron chelator, and chloroquine against hemin peroxidation (Sonnet and Mullie, 2011).

Quinoline-based drugs, like chloroquine, are weak bases known to accumulate in acidic vacuoles. This ion trapping model of action is one mechanism proposed in the treatment of malaria, where chloroquine-heme accumulation within the digestive vacuole of the *Plasmodium* spp. enhances drug activity (Foley and Tilley, 1998). Although a putative heme oxygenase enzyme has been identified in

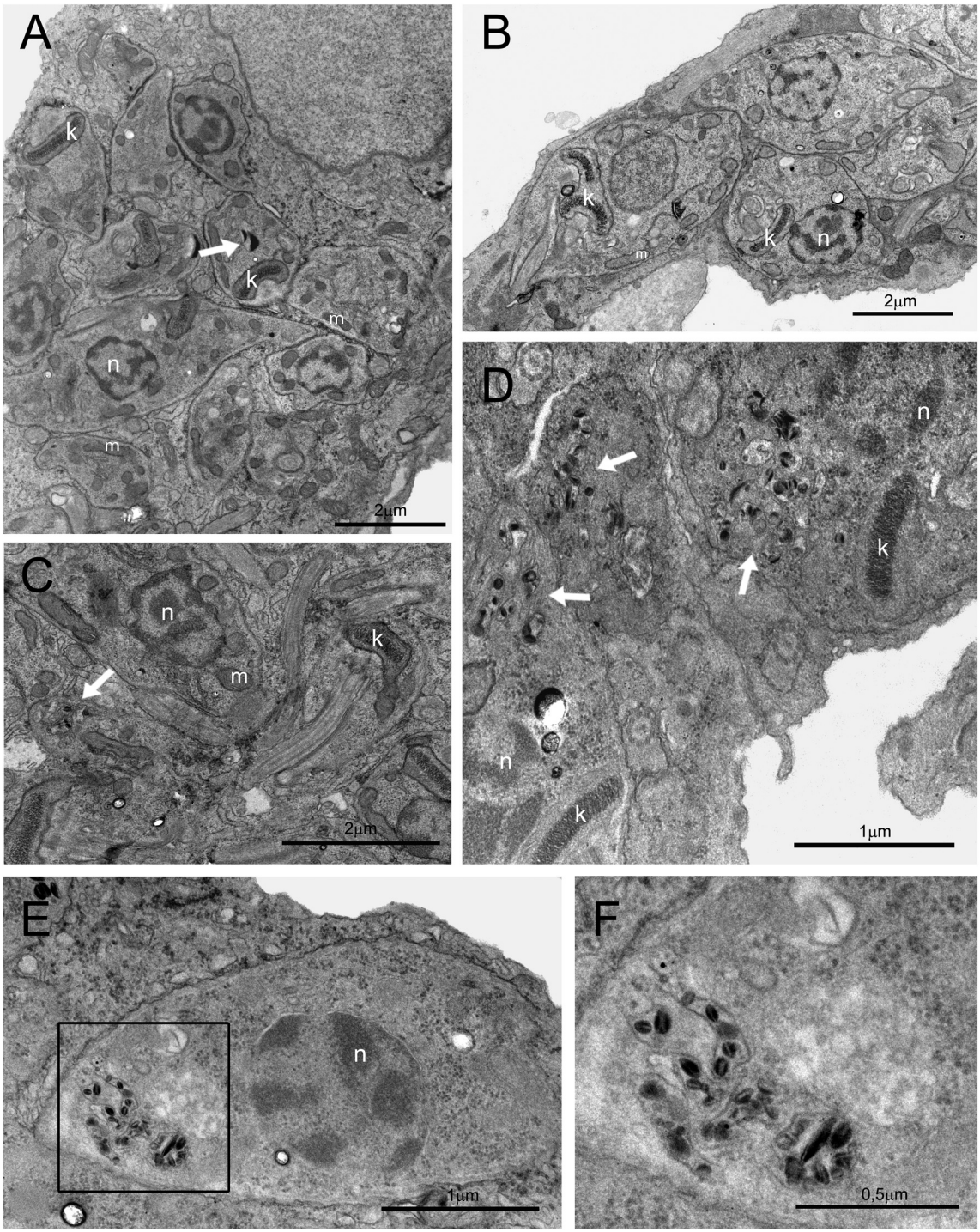

Fig. 6. Ultrastructural analysis of *T. cruzi*-infected cardiomyocytes treated with quinoline 1**g** combined with heme. (A) Untreated infected cardiomyocytes after 96 h show intracellular forms with preserved mitochondria (m), nucleus (n), bar-shaped kinetoplast (k) and structures that resemble reservosome with a electron dense portion limited by a membrane (arrow). (B) Hemin (30 μM) treated cardiomyocytes shows intracellular amastigotes with kinetoplast (k) under division and unaltered mitochondria (m) and nucleus (n). (C) Infected cultures incubated with 30 μM of hemin and 1**g** (IC50) for 72 h. Intracellular forms show preserved intracellular organelles and electron-dense granules in vesicles within the parasite (arrow). (D and E) Infected cardiomyocytes treated with 1**g** (IC75) in combination with hemin (30 μM) for 72 h revealed no alteration in nucleus (n) and kinetoplast (k), but an increased number of reservosomes with electron-dense deposit in posterior region of parasites was observed (arrow). (F) High magnification shows reservosomes with electron-dense inclusion with membrane profiles. (A, B and C) Bars = 2 μm; (D and E) Bars = 1 μm (F) Bars = 0.5 μm.

the genome of *Plasmodium* spp. (Sigala et al., 2012), this parasite lacks the active enzyme preventing the cleavage of free heme released by the proteolysis of hemoglobin but, instead, heme detoxification occurs mainly by its crystallization into non-toxic hemozoin (Gorka et al., 2013). Thus, association of quinoline drugs with heme, which seems to be essential for chloroquine uptake (Bray et al., 1999), inhibits the hemozoin formation in the digestive vacuole.

Interestingly, the detection of a heme oxygenase-like enzyme in *T. cruzi* (Cupello et al., 2014) indicates a different heme catabolism

pathway compared to the *Plasmodium* spp. Although the complete pathway is still unknown, results showed a rapid uptake of heme via the ABC transporter (Cupello et al., 2011), that reaches the reservosome, an acid compartment that stores lipids and proteases (Cunha-e-Silva et al., 2006). Our ultrastructural data demonstrated that combined treatment (hemin and compound 1**g**) induced an increase of electron-dense deposits and membrane profiles within reservosomes in intracellular forms. Electron density and membranous structures have been largely described in lysosome-related organelles and reservosomes (Cunha-e-Silva et al., 2006; Sant'Anna et al., 2008). This finding is also in accordance with previous report that demonstrated heme and iron accumulation in electron-dense vesicles in midgut epithelial cells of *Rhodnius prolixus*, identified as haemoxisome (Roberto Silva et al., 2006). Recently, it has also been shown an electron density in reservosome associated with hemin storage (da Silva Augusto et al., 2015). Additionally, it has been described a transmembrane *T. cruzi* heme transporter enhancer protein (TcHTE), localized in flagellar pocket of epimastigotes, responsible for heme uptake (Merli et al., 2016). High-performance liquid chromatography analysis showed that heme is enzymatically catabolized in biliverdin, supporting the heme oxygenase activity in *T. cruzi* (Cupello et al., 2014). Thus, the formation of heme-quinoline 1**g** complex may inhibit heme degradation and, therefore, increase trypanocidal activity.

Furthermore, the heme-quinoline interaction can play a dual role in *T. cruzi* infection, acting on the pathway of heme catabolism of the parasite and modulating the host immune response. The combination of compounds (heme and quinoline) can trigger a reduction in available heme levels, leading to the activation of TcK2, a kinase recently reported to phosphorylate eIF2α that inhibits proliferation and induces differentiation of the parasite (da Silva Augusto et al., 2015). Another possibility is that the formation of the complex increases the production of reactive oxygen species, leading to cytotoxicity and parasite damage. Based on our observation that treatment with combined substances induced necrosis of the parasite, we propose a mechanism of action involving toxic intermediates, leading to pro-oxidant effects and parasite death as previously described in malaria parasites (Loria et al., 1999).

Regulation of the host immune response has been recently reported by activation of heme oxygenase in a murine model of *T. cruzi* infection (Gutierrez et al., 2014). Although treatment of *T. cruzi* infected mice with hemin, a HO-1 inducer, has not improved the survival of the mice, it was able to reduce the levels of parasitemia and heart inflammation. Thus, the combined treatment of quinoline derivatives and heme may modulate the immune and inflammatory response in addition to potentiate free radicals production in the parasites. In accordance to this hypothesis, the ultrastructural analysis demonstrated a drastic effect in kDNA and mitochondria. Similar drug effects have been shown in response to treatment with quinone derivatives, substances that induce the formation of free radicals that damage mainly the parasite mitochondria, due to the lack of efficient mechanism for ROS detoxification (Salomão et al., 2013). Another striking result was that the combined treatment induced duplication of axonemes in trypomastigotes, a non-proliferative form of *T. cruzi*. This peculiar event has also been reported in trypomastigotes treated with diamidine (DB1670), a nitrogen heterocyclic compound that binds to DNA's minor groove, showing a potent trypanocidal effect (Batista et al., 2010).

A remarkable clinical application for heme administration is photodynamic therapy (PDT). The basis of this therapy lies in the treatment of cells with the heme precursor, δ-aminolevulinic acid (ALA) that boosts cellular endogenous heme biosynthesis. This protoporphyrin IX (PpIX) acts as a photosensitizer that produces ROS after laser beam excitation. ALA-induced PDT has been extensively used in the treatment of non-melanoma skin cancer (Ohgari et al., 2011) and leishmaniasis (Gardlo et al., 2003; Sohl et al., 2007). PDT has considerable successful rates in treating these diseases because PpIX accumulates preferentially in tumor tissues and leishmaniasis cutaneous lesions. A promising synergistic mechanism involves quinolone derivatives that enhanced PpIX accumulation and phototoxicity of tumor cells after ALA-induced PDT (Ohgari et al., 2011). Furthermore, the inhibition of HO-1 by Sn-protoporphyrin increased PpIX accumulation and sensitivity of neoplasic cells, improving ALA-PDT treatment of cancer (Frank et al., 2007). Additionally, the combination of extracellular heme with the antimalarial drug artemisinin enhanced the oxidative effect of heme (Tangnitipong et al., 2012). Thus, endogenous stimulation of heme by ALA and exogenous addition of protoporphyrin IX and holotransferrin, improved cytotoxicity of dihydroartemisinin in cancer cells (Zhang and Gerhard, 2009). These results showed that diverse strategies to regulate heme levels can modulate the drug activity.

The trypanocidal activity of this series of 4-aminoquinolines and the elucidation of the mechanism involving interactions with heme is an open field of research that can improve and guide rational drug development and combination strategies. Targeting heme uptake, transport and catabolic pathways are a promising alternative mechanism to fight Chagas disease, considering the parasite's lack of heme biosynthetic pathway and the essential need of this molecule for parasite homeostasis.

Conflict of interest

The authors declare that they have no competing interests.

Funding information

This work was supported by grants from Fundação Oswaldo Cruz/Conselho Nacional de Desenvolvimento Científico e Tecnológico (FIOCRUZ/CNPq; grant 7190637612315942 to Mirian C.S. Pereira; MCTI/Universal, grant 480328/2013-7 to Claudia M. Calvet), Fundação de Amparo à Pesquisa do Estado do Rio de Janeiro (FAPERJ; grant E-26/010.001548/2014 to Mirian C.S. Pereira) and Programa Estratégico de Apoio à Pesquisa em Saúde (PAPES; grant 4051089454296667 to Mirian C. S. Pereira).

Acknowledgments

The authors thank the Platform of Electron Microscopy of Institute Oswaldo Cruz and Platform of Bioassay for use of their facilities and Renata Soares Dias de Souza for technical support. We also would like to thank Dr. Norman A. Ratcliffe for his careful reading and relevant contribution for the manuscript.

Appendix A. Supplementary data

Supplementary data related to this article can be found at http://dx.doi.org/10.1016/j.ijpddr.2016.07.001.

References

Alves, E., Iglesias, B.A., Deda, D.K., Budu, A., Matias, T.A., Bueno, V.B., Maluf, F.V., Guido, R.V.C., Oliva, G., Catalani, L.H., Araki, K., Garcia, C.R.S., 2015. Encapsulation of metalloporphyrins improves their capacity to block the viability of the human malaria parasite Plasmodium falciparum. Nanomedicine 11, 351–358. http://dx.doi.org/10.1016/j.nano.2014.09.018.

Batista, D.G.J., Pacheco, M.G.O., Kumar, A., Branowska, D., Ismail, M.A., Hu, L., Boykin, D.W., Soeiro, M.N.C., 2010. Biological, ultrastructural effect and subcellular localization of aromatic diamidines in Trypanosoma cruzi. Parasitology 137, 251–259. http://dx.doi.org/10.1017/S0031182009991223.

Borges, J.C., Carvalho, A.V., Bernardino, A.M.R., Oliveira, C.D., Pinheiro, L.C.S.,

Marra, R.K.F., Castro, H.C., Wardell, S.M.S.V., Wardell, J.L., Amaral, V.F., Canto-Cavalheiro, M.M., Leon, L.L., Genestra, M., 2014. Synthesis and in vitro evaluation of new benzenesulfonamides as antileishmanial agents. J. Braz. Chem. Soc. 25, 980–986. http://dx.doi.org/10.5935/0103-5053.20140062.

Bray, P.G., Janneh, O., Ward, S.A., 1999. Chloroquine uptake and activity is determined by binding to ferriprotoporphyrin IX in Plasmodium falciparum. Novartis Found. Symp. 226, 252–260 discussion 260–264.

Carneiro, P.F., do Nascimento, S.B., Pinto, A.V., Pinto Mdo, C., Lechuga, G.C., Santos, D.O., dos Santos Jr., H.M., Resende, J.A., Bourguignon, S.C., Ferreira, V.F., 2012. New oxirane derivatives of 1,4-naphthoquinones and their evaluation against *T. cruzi* epimastigote forms. Bioorg. Med. Chem. 20, 4995–5000. http://dx.doi.org/10.1016/j.bmc.2012.06.027.

Choi, J.Y., Calvet, C.M., Gunatilleke, S.S., Ruiz, C., Cameron, M.D., McKerrow, J.H., Podust, L.M., Roush, W.R., 2013. Rational development of 4-aminopyridyl-based inhibitors targeting trypanosoma cruzi CYP51 as anti-chagas agents. J. Med. Chem. 56, 7651–7668. http://dx.doi.org/10.1021/jm401067s.

Conteh, L., Engels, T., Molyneux, D.H., 2010. Socioeconomic aspects of neglected tropical diseases. Lancet 375, 239–247. http://dx.doi.org/10.1016/S0140-6736(09)61422-7.

Coura, J.R., Castro, S.L. de, 2002. A critical review on chagas disease chemotherapy. Mem. Inst. Oswaldo Cruz 97, 3–24.

Coura, J.R., Vinas, P.A., 2010. Chagas disease: a new worldwide challenge. Nature 465, S6–S7. http://dx.doi.org/10.1038/nature09221.

Cunha-e-Silva, N., Sant'Anna, C., Pereira, M.G., Porto-Carreiro, I., Jeovanio, A.L., de Souza, W., 2006. Reservosomes: multipurpose organelles? Parasitol. Res. 99, 325–327. http://dx.doi.org/10.1007/s00436-006-0190-3.

Cupello, M.P., Souza, C.F., Buchensky, C., Soares, J.B., Laranja, G.A., Coelho, M.G., Cricco, J.A., Paes, M.C., 2011. The heme uptake process in Trypanosoma cruzi epimastigotes is inhibited by heme analogues and by inhibitors of ABC transporters. Acta Trop. 120, 211–218. http://dx.doi.org/10.1016/j.actatropica.2011.08.011.

Cupello, M.P., Souza, C.F., Menna-Barreto, R.F., Nogueira, N.P., Laranja, G.A., Sabino, K.C., Coelho, M.G., Oliveira, M.M., Paes, M.C., 2014. Trypanosomatid essential metabolic pathway: new approaches about heme fate in Trypanosoma cruzi. Biochem. Biophys. Res. Commun. 449, 216–221. http://dx.doi.org/10.1016/j.bbrc.2014.05.004.

da Silva Augusto, L., Moretti, N.S., Ramos, T.C., de Jesus, T.C., Zhang, M., Castilho, B.A., Schenkman, S., 2015. A membrane-bound eIF2 alpha kinase located in endosomes is regulated by heme and controls differentiation and ROS levels in Trypanosoma cruzi. PLoS Pathog. 11, e1004618. http://dx.doi.org/10.1371/journal.ppat.1004618.

de Menezes, D.D., Calvet, C.M., Rodrigues, G.C., de Souza Pereira, M.C., Almeida, I.R., de Aguiar, A.P., Supuran, C.T., Vermelho, A.B., 2015. Hydroxamic acid derivatives: a promising scaffold for rational compound optimization in Chagas disease. J. Enzym. Inhib. Med. Chem. 1–10. http://dx.doi.org/10.3109/14756366.2015.1077330.

Don, R., Ioset, J.R., 2014. Screening strategies to identify new chemical diversity for drug development to treat kinetoplastid infections. Parasitology 141, 140–146. http://dx.doi.org/10.1017/S003118201300142X.

Egan, T.J., 2006. Interactions of quinoline antimalarials with hematin in solution. J. Inorg. Biochem. 100, 916–926. http://dx.doi.org/10.1016/j.jinorgbio.2005.11.005.

Eswaran, S., Adhikari, A.V., Chowdhury, I.H., Pal, N.K., Thomas, K.D., 2010. New quinoline derivatives: synthesis and investigation of antibacterial and antituberculosis properties. Eur. J. Med. Chem. 45, 3374–3383. http://dx.doi.org/10.1016/j.ejmech.2010.04.022.

Foley, M., Tilley, L., 1998. Quinoline antimalarials: mechanisms of action and resistance and prospects for new agents. Pharmacol. Ther. 79, 55–87. http://dx.doi.org/10.1016/s0163-7258(98)00012-6.

Fonseca-Berzal, C., Rojas Ruiz, F.A., Escario, J.A., Kouznetsov, V.V., Gomez-Barrio, A., 2014. In vitro phenotypic screening of 7-chloro-4-amino(oxy)quinoline derivatives as putative anti-Trypanosoma cruzi agents. Bioorg. Med. Chem. Lett. 24, 1209–1213. http://dx.doi.org/10.1016/j.bmcl.2013.12.071.

Frank, J., Lornejad-Schafer, M.R., Schoffl, H., Flaccus, A., Lambert, C., Biesalski, H.K., 2007. Inhibition of heme oxygenase-1 increases responsiveness of melanoma cells to ALA-based photodynamic therapy. Int. J. Oncol. 31, 1539–1545.

Ganguly, A., Banerjee, K., Chakraborty, P., Das, S., Sarkar, A., Hazra, A., Banerjee, M., Maity, A., Chatterjee, M., Mondal, N.B., Choudhuri, S.K., 2011. Overcoming multidrug resistance (MDR) in cancer in vitro and in vivo by a quinoline derivative. Biomed. Pharmacother. 65, 387–394. http://dx.doi.org/10.1016/j.biopha.2011.04.024.

Gardlo, K., Horska, Z., Enk, C.D., Rauch, L., Megahed, M., Ruzicka, T., Fritsch, C., 2003. Treatment of cutaneous leishmaniasis by photodynamic therapy. J. Am. Acad. Dermatol 48, 893–896. http://dx.doi.org/10.1067/mjd.2003.218.

Gorka, A.P., de Dios, A., Roepe, P.D., 2013. Quinoline drug-heme interactions and implications for antimalarial cytostatic versus cytocidal activities. J. Med. Chem. 56, 5231–5246. http://dx.doi.org/10.1021/jm400282d.

Gutierrez, F.R., Pavanelli, W.R., Medina, T.S., Silva, G.K., Mariano, F.S., Guedes, P.M., Mineo, T.W., Rossi, M.A., Cunha, F.Q., Silva, J.S., 2014. Haeme oxygenase activity protects the host against excessive cardiac inflammation during experimental Trypanosoma cruzi infection. Microbes Infect. 16, 28–39. http://dx.doi.org/10.1016/j.micinf.2013.10.007.

Jimenez, V., 2014. Dealing with environmental challenges: mechanisms of adaptation in Trypanosoma cruzi. Res. Microbiol. 165, 155–165. http://dx.doi.org/10.1016/j.resmic.2014.01.006.

Kinnamon, K.E., Poon, B.T., Hanson, W.L., Waits, V.B., 1996. Primaquine analogues that are potent anti-Trypanosoma cruzi agents in a mouse model. Ann. Trop. Med. Parasitol. 90, 467–474.

Krishnamurthy, P., Xie, T., Schuetz, J.D., 2007. The role of transporters in cellular heme and porphyrin homeostasis. Pharmacol. Ther. 114, 345–358. http://dx.doi.org/10.1016/j.pharmthera.2007.02.001.

Lara, F.A., Sant'Anna, C., Lemos, D., Laranja, G.A.T., Coelho, M.G.P., Reis Salles, I., Michel, a., Oliveira, P.L., Cunha-e-Silva, N., Salmon, D., Paes, M.C., 2007. Heme requirement and intracellular trafficking in Trypanosoma cruzi epimastigotes. Biochem. Biophys. Res. Commun. 355, 16–22. http://dx.doi.org/10.1016/j.bbrc.2006.12.238.

Leal, B., Afonso, I.F., Rodrigues, C.R., Abreu, P.A., Garrett, R., Pinheiro, L.C.S., Azevedo, A.R., Borges, J.C., Vegi, P.F., Santos, C.C.C., da Silveira, F.C.A., Cabral, L.M., Frugulhetti, I.C.P.P., Bernardino, A.M.R., Santos, D.O., Castro, H.C., 2008. Antibacterial profile against drug-resistant Staphylococcus epidermidis clinical strain and structure-activity relationship studies of 1H-pyrazolo[3,4-b]pyridine and thieno[2,3-b]pyridine derivatives. Bioorg. Med. Chem. 16, 8196–8204. http://dx.doi.org/10.1016/j.bmc.2008.07.035.

Leed, A., DuBay, K., Ursos, L.M.B., Sears, D., De Dios, A.C., Roepe, P.D., 2002. Solution structures of antimalarial drug-heme complexes. Biochemistry 41, 10245–10255. http://dx.doi.org/10.1021/bi020195i.

Loria, P., Miller, S., Foley, M., Tilley, L., 1999. Inhibition of the peroxidative degradation of haem as the basis of action of chloroquine and other quinoline antimalarials. Biochem. J. 339 (Pt 2), 363–370. http://dx.doi.org/10.1042/0264-6021:3390363.

Meeks, B., Melacini, P.R., Pogue, J., Mattos, A., Lazdins, J., Rassi, A., Connolly, S.J., 2015. Randomized trial of benznidazole for chronic chagas' cardiomyopathy. N. Engl. J. Med. 373, 1295–1306. http://dx.doi.org/10.1056/NEJMoa1507574.

Meirelles, M.N., de Araujo-Jorge, T.C., Miranda, C.F., de Souza, W., Barbosa, H.S., 1986. Interaction of Trypanosoma cruzi with heart muscle cells: ultrastructural and cytochemical analysis of endocytic vacuole formation and effect upon myogenesis in vitro. Eur. J. Cell Biol. 41, 198–206.

Meirelles, M.N., Souto-Padron, T., De Souza, W., 1984. Participation of cell surface anionic sites in the interaction between Trypanosoma cruzi and macrophages. J. Submicrosc. Cytol. 16, 533–545.

Merli, M.L., Pagura, L., Hernández, J., Barisón, M.J., Pral, E.M.F., Silber, A.M., Cricco, J.A., 2016. The trypanosoma cruzi protein TcHTE is critical for heme uptake. PLoS Negl. Trop. Dis. 10, e0004359. http://dx.doi.org/10.1371/journal.pntd.0004359.

Molina, I., Salvador, F., Sanchez-Montalva, A., 2014. Posaconazole versus benznidazole for chronic Chagas' disease. N. Engl. J. Med. 371, 966. http://dx.doi.org/10.1056/NEJMc1407914.

Muscia, G.C., Cazorla, S.I., Frank, F.M., Borosky, G.L., Buldain, G.Y., Asis, S.E., Malchiodi, E.L., 2011. Synthesis, trypanocidal activity and molecular modeling studies of 2-alkylaminomethylquinoline derivatives. Eur. J. Med. Chem. 46, 3696–3703. http://dx.doi.org/10.1016/j.ejmech.2011.05.035.

Nakayama, H., Desrivot, J., Bories, C., Franck, X., Figadère, B., Hocquemiller, R., Fournet, A., Loiseau, P.M., 2007. In vitro and in vivo antileishmanial efficacy of a new nitrilquinoline against Leishmania donovani. Biomed. Pharmacother. 61, 186–188. http://dx.doi.org/10.1016/j.biopha.2007.02.001.

Ohgari, Y., Miyata, Y., Chau, T.T., Kitajima, S., Adachi, Y., Taketani, S., 2011. Quinolone compounds enhance delta-aminolevulinic acid-induced accumulation of protoporphyrin IX and photosensitivity of tumour cells. J. Biochem. 149, 153–160. http://dx.doi.org/10.1093/jb/mvq126.

Pham, N.K., Mouriz, J., Kima, P.E., 2005. Leishmania pifanoi amastigotes avoid macrophage production of superoxide by inducing heme degradation. Infect. Immun. 73, 8322–8333. http://dx.doi.org/10.1128/IAI.73.12.8322-8333.2005.

Rassi, A., Marin-Neto, J.A., 2010. Chagas disease. Lancet 375, 1388–1402. http://dx.doi.org/10.1016/S0140-6736(10)60061-X.

Roberto Silva, J., Gomes-Silva, L., Casado Lins, U., Nogueira, N.F.S., Dansa-Petretski, M., 2006. The haemoxisome: a haem-iron containing structure in the Rhodnius prolixus midgut cells. J. Insect Physiol. 52, 542–550. http://dx.doi.org/10.1016/j.jinsphys.2006.01.004.

Salomão, K., De Santana, N.A., Molina, M.T., De Castro, S.L., Menna-Barreto, R.F., 2013. Trypanosoma cruzi mitochondrial swelling and membrane potential collapse as primary evidence of the mode of action of naphthoquinone analogues. BMC Microbiol. 13, 196. http://dx.doi.org/10.1186/1471-2180-13-196.

Sant'Anna, C., Parussini, F., Lourenço, D., De Souza, W., Cazzulo, J.J., Cunha-E-Silva, N.L., 2008. All Trypanosoma cruzi developmental forms present lysosome-related organelles. Histochem. Cell Biol. 130, 1187–1198. http://dx.doi.org/10.1007/s00418-008-0486-8.

Sigala, P.A., Crowley, J.R., Hsieh, S., Henderson, J.P., Goldberg, D.E., 2012. Direct tests of enzymatic heme degradation by the malaria parasite Plasmodium falciparum. J. Biol. Chem. 287, 37793–37807. http://dx.doi.org/10.1074/jbc.M112.414078.

Sohl, S., Kauer, F., Paasch, U., Simon, J.C., 2007. Photodynamic treatment of cutaneous leishmaniasis. J. Dtsch. Dermatol. Ges. 5, 128–130. http://dx.doi.org/10.1111/j.1610-0387.2007.06177.x.

Sonnet, P., Mullie, C., 2011. In vitro antimalarial activity of ICL670: a further proof of the correlation between inhibition of beta-hematin formation and of peroxidative degradation of hemin. Exp. Parasitol. 128, 26–31. http://dx.doi.org/10.1016/j.exppara.2011.01.018.

Tangnitipong, S., Thaptimthong, T., Srihirun, S., Unchern, S., Kittikool, D., Udomsangpetch, R., Sibmooh, N., 2012. Extracellular heme enhances the antimalarial activity of artemisinin. Biol. Pharm. Bull. 35, 29–33. http://dx.doi.org/10.1248/bpb.35.29.

Tekwani, B.L., Walker, L.A., 2006. 8-Aminoquinolines: future role as antiprotozoal drugs. Curr. Opin. Infect. Dis. 19, 623–631. http://dx.doi.org/10.1097/QCO.0b013e328010b848.

Tiuman, T.S., Santos, A.O., Ueda-Nakamura, T., Filho, B.P.D., Nakamura, C.V., 2011. Recent advances in leishmaniasis treatment. Int. J. Infect. Dis. 15, 525–532. http://dx.doi.org/10.1016/j.ijid.2011.03.021.

Tripodi, K.E., Menendez Bravo, S.M., Cricco, J.A., 2011. Role of heme and heme-proteins in trypanosomatid essential metabolic pathways. Enzym. Res. 2011, 873230. http://dx.doi.org/10.4061/2011/873230.

Upadhayaya, R.S., Dixit, S.S., Foldesi, A., Chattopadhyaya, J., 2013. New antiprotozoal agents: their synthesis and biological evaluations. Bioorg. Med. Chem. Lett. 23, 2750–2758. http://dx.doi.org/10.1016/j.bmcl.2013.02.054.

Vannucchi, V., Tomberli, B., Zammarchi, L., Fornaro, A., Castelli, G., Pieralli, F., Berni, A., Yacoub, S., Bartoloni, A., Olivotto, I., 2014. Chagas disease as a cause of heart failure and ventricular arrhythmias in patients long removed from endemic areas: an emerging problem in Europe. J. Cardiovasc Med. http://dx.doi.org/10.2459/JCM.0000000000000045.

WHO, 2015. Chagas disease (American trypanosomiasis) [WWW document]. World Heal. Organ. http://www.who.int/mediacentre/factsheets/fs340/en/.

Zhang, S., Gerhard, G.S., 2009. Heme mediates cytotoxicity from artemisinin and serves as a general anti-proliferation target. PLoS One 4, e7472. http://dx.doi.org/10.1371/journal.pone.0007472.